LAWRENCE
LIVERMORE
NATIONAL
LABORATORY

LLNL-PROC-410546

Electrical Transport Experiments at High Pressure

S. Weir

February 13, 2009

SUSSP 2008: High Pressure Physics
Skye, United Kingdom
May 26, 2008 through June 6, 2008

Disclaimer

Electrical Transport Experiments at High Pressure

S.T. Weir

High-pressure electrical measurements have a long history of use in the study of materials under ultra-high pressures. In recent years, electrical transport experiments have played a key role in the study of many interesting high pressure phenomena including pressure-induced superconductivity, insulator-to-metal transitions, and quantum critical behavior. High-pressure lectrical transport experiments also play an important function in geophysics and the study of the Earth's interior.

Besides electrical conductivity measurements, electrical transport experiments also encompass techniques for the study of the optoelectronic and thermoelectric properties of materials under high pressures. In addition, electrical transport techniques, i.e., the ability to extend electrically conductive wires from outside instrumentation into the high pressure sample chamber have been utilized to perform other types of experiments as well, such as high-pressure magnetic susceptibility and de Haas – van Alphen Fermi surface experiments. Finally, electrical transport techniques have also been utilized for delivering significant amounts of electrical power to high pressure samples, for the purpose of performing high-pressure and –temperature experiments. Thus, not only do high-pressure electrical transport experiments provide much interesting and valuable data on the physical properties of materials extreme compression, but the underlying high-pressure electrical transport techniques can be used in a number of ways to develop additional diagnostic techniques and to advance high pressure capabilities.

Electrical Measurement Techniques with Diamond Anvil Cells

Electrical transport experiments with diamond anvil cells (DAC's) are very challenging. Because of the very small sample sizes involved and because of the presence of a metal pressure gasket in most experiments, signal wires leading to the high-pressure sample must be well insulated to avoid short-circuits. A large number of different approaches have been developed over the years to address this key problem. One solution is to replace the metal gasket with an insulating gasket. Mica-MgO composite gaskets, for example, have been successfully used to 40 GPa [1]. The metal gasket can also be coated with an electrically insulating layer by either sputtering [2], plasma-spraying [1], or by coating the gasket with mixture of alumina or cubic boron nitride mixed with epoxy [3]. (Figure 1)

Several approaches have also been used to make the electrically conductive paths to the high-pressure sample. Fine metal wires (<25 μm diameter) or very flat metal foils of gold or platinum are often used. Recent years have also seen the development and application of a variety of advanced microfabrication techniques for placing electrically conductive paths on or within the diamond anvils themselves [4,5,6,7]. These include the use of boron implantation, focused ion beam (FIB) equipment, and the combined use of microlithography and diamond chemical vapor deposition (CVD).

Electrical contacts between the sample and the conductive wires can be made in several ways. Simple pressed contacts are often sufficient to ensure good electrical contact between the wires and the sample, provided that the sample's surfaces are clean

of oxide or contamination layers. In situations where secure contacts are required, small amounts of silver paste or silver epoxy can be used to bond the wire to the sample. These contacts may be applied directly to the sample, but contact resistances can often be reduced if thin-film metal contact pads (e.g., Au, Pt) are first evaporated or sputter deposited onto the sample. If the sample is a semiconductor, depositing metal contact films onto it is also beneficial since this will tend to reduce the tendency for the metal-to-semiconductor contacts to be rectifying (or "Shottky") contacts. Generally, non-rectifying or "ohmic" contacts are desirable for delivering electrical currents to semiconductors and getting voltage signals out of them. Finally, laser welding or spark welding have occasionally been used to make contacts to samples. The drawback with these methods is that special equipment is needed to deal with DAC-sized samples, and that special care must be taken to avoid overheating the sample.

The van der Pauw method [8] is frequently used for measuring the resistivity of arbitrarily shaped samples. There are several requirements associated with the van der Pauw method: the contacts to the sample must be located on the boundary of the sample, the contact areas should be small in comparison to the sample size, and the sample should be of some known uniform thickness. If these conditions are satisfied, the van der Pauw method is a powerful technique for determining the sample resistivity of samples of arbitrary shape (subject to the restriction that the thickness is uniform and known). If small electrical contacts are made at four points *A*, *B*, *C*, and *D*, on the periphery of the sample, a current I_{AB} can be applied from contact *A* to contact *B* while measuring the voltage drop V_D-V_C. If we define $R_{AB,CD}= (V_D-V_C)/I_{AB}$ and, analogously, $R_{BC,DA}=(V_A-V_D)/I_{BC}$ then the resistivity ρ is given by the equation [8]

$$\exp\left(-\frac{\pi d}{\rho}R_{AB,CD}\right)+\exp\left(-\frac{\pi d}{\rho}R_{BC,DA}\right)=1 \qquad \text{(Eqn 1)}$$

The resistivity ρ cannot be solved for as a closed–form expression from this equation, but the resistivity can be calculated by numerical methods for any given $R_{AB,CD}$ and $R_{BC,DA}$. The equation is simplified considerably if the points of electrical contact are symmetrically arranged around the circumference of a disc of uniform resistivity, then $R_{AB,CD}= R_{BC,DA}$ and eqn. 1 reduces to

$$\rho=\frac{\pi d}{\ln(2)}R_{AB,CD} \qquad \text{(Eqn. 2)}$$

In practice, however, the van der Pauw method, is usually difficult to apply to DAC resistivity experiments. The contact areas are often a significant fraction of the sample size, the samples are often completely irregular in shape, and the *in situ* thickness of a high pressure is usually very difficult to determine with much accuracy. However, a rough estimate of the absolute resistivity can usually be made based on the sample dimensions and the locations of the contact points by using 4-wire resistance

measurements. The absolute resistivity of the sample can also be estimated by simulating the 3D current flow through the sample using the actual sample geometry and the positions of the probes on the sample [9].

Superconductivity under High Pressures

The study of superconductivity under high pressures is motivated by both scientific and technological concerns. The dependence of the superconducting transition temperature on applied pressure can be used to test and confirm theories. The behavior of the transition temperature on applied pressure can also be used to focus efforts to develop new superconductors with higher transition temperatures. A superconductor which exhibits a relatively high transition temperature under high pressures, for example, is an obvious candidate for further study to see if higher transition temperatures can also be achieved by applying "chemical pressure" through selective impurity doping of its lattice.

Iron

The appearance of superconductivity in iron might thought to be unlikely since ferromagnetism and superconductivity are expected to be mutually exclusive according to conventional BCS theory. Strong magnetic fields tend to align the spins of each Cooper electron pair in the same direction and thus break up the Cooper pairs. Above 10 GPa, however, iron transforms to a non-magnetic structure, and conventional superconductivity becomes a possibility at low temperatures. Shimizu, et. al. [10], performed high-pressure electrical conductivity experiments on high purity iron samples by using an arrangement of gold and platinum foils and wires, with a thin layer of alumina covering the metal gasket for electrical insulation. NaCl, which is much weaker than alumina, was used as the pressure medium to cushion the iron sample. Spot welding was used to securely attach gold electrodes to the sample (Figure 2a). A sharp 10% drop in the resistance associated with the appearance of superconductivity is clearly seen at a temperature of approximately 1K at a pressure of 25 GPa. (Figure 2b). The fact that the resistance does not drop entirely to zero could be due to pressure inhomogeneities in the sample, or small contact resistances in the gold-to-iron spot welds.

The magnetic field dependence of the resistivity behavior confirms the existence of superconductivity in the iron sample. Figure 3 shows that the resistivity drop decreases with increasing magnetic field, until superconductivity is entirely quenched at a magnetic field of 1.8 Tesla. Finally, Figure 4 shows the pressure dependence of the superconducting transition discovered between 15 and 30 GPa.

Oxygen

Based on high-pressure optical absorption edge and reflectivity experiments [11], oxygen metallizes at approximately 95 GPa. The transition from insulating molecular oxygen to metallic molecular oxygen is accompanied by a structural phase transition. Shimizu, et. al. [12], performed electrical conductivity experiments and discovered superconductivity in solid molecular oxygen in the pressure range from 98 GPa to at least 125 GPa. Figure 5 shows the preparation of the sample chamber, with four platinum foil

electrodes contacting the oxygen sample. Figure 6 shows the magnetic field dependence of the resistance transition, and confirms the existence of superconductivity with a critical field of about 0.2 Tesla at 120 GPa.

Conductivity Experiments at High-Pressure and Very High Temperatures

Relatively little work has been performed involving DAC electrical conductivity measurements at conditions of high pressures and very high temperatures (>> 1000 ˚C), a temperature regime where externally heated DAC's start to give way to laser-heated DAC's and internal resistive heating techniques. Pioneering work on using internal resistive heating to heat tiny iron wires in a DAC while monitoring changes in the resistances of the wires was performed by Liu and Bassett [13], Mao, et. al. [14], and Boehler, et. al. [15]. In all these experiments, very fine iron wires with diameters ranging from 5 to 20 μm were heated by driving large electrical currents through them. Typical currents were in the 1-3 ampere range for a power dissipation in the range of a few watts and temperatures up to 2500 K.

Knittle and Jeanloz [16] performed electrical conductivity experiments on a laser heated FeO sample at pressures of about 70 GPa and temperatures of over 1000 ˚C, and confirmed the existence of a metallic phase of FeO under simultaneous conditions of high-pressure and –temperature which was first identified with shock-wave experiments. More recently, Li, et. al., [17] have performed conductivity measurements on high-pressure, laser-heated samples of $(Fe_{0.125}, Mg_{0.875})_2SiO_4$ using a specially prepared diamond anvil with an electrical thin-film circuit and a 3 μm thick alumina thermal insulating layer on it.

Single Crystal Experiments

Electrical transport experiments on single crystal samples require special care and preparation due to the need to avoid excessive shearing stresses on the sample while at the same time maintaining secure electrical connections to the sample. Electrical connections may be made by using silver or gold paint or epoxy to bond thin wires to the sample. In order to provide good ohmic contacts to some samples, thin film pads of gold may need to be sputter deposited onto the sample before bonding wires to it. Either photolithographic masking or shadow masking can be used to prepare the sample for sputter deposition.

A good pressure medium is needed to minimize shearing stresses on the sample. Ideally, the medium should remain fluid to very high pressures and possess a very small strength even after it solidifies. Additionally, it should be chemically inert and not react with either the sample or the metal wires. Thermal stability and non-toxicity are also desirable properties. Methanol-ethanol mixtures, Fluorinert 3M, argon, and helium are commonly used media.

The inset of Figure 7a shows the setup of an electrical conductivity experiment by Cui, et. al. [18] on a single crystal sample of an organic semiconductor, tetramethyltetratelluronaphtalene (TMTTeN). Four thin gold wires (5 μm diameter) were attached to the sample with gold paint, and a fluorocarbon mixture of Fluorinert 3M,

FC70, and FC72 was used as a pressure medium. Figure 7b shows the resistivity as a function of temperature for pressures up to 25.4 GPa, at which point the activation energy for conduction has been reduced to about 5 meV.

Hall Effect and Magnetoresistance

Hall effect and magnetoresistance experiments have been performed on single crystal and thin-film samples in diamond anvil cells. Hall effect experiments are useful for measuring the charge carrier density and also giving information on the sign of the charge carriers. The Hall coefficient is defined by

$$R_H = E_y/(j_x B) = V_H/(IB/d)$$

Where E_y is the transverse electric field, j_x is the current density, B is the magnetic field, V_H is the Hall voltage, I is the current, and d is the sample thickness. For materials in which the electric current is carried by a single band, if *n* is the density of carriers and *e* is the electron charge then the Hall coefficient is –(1/ne) or +(1/ne), depending on whether the current is carried by electrons or holes, respectively. For semiconductors in which both electrons and holes may be present the Hall coefficient is

$$R_H = \frac{-n\mu_e^2 + p\mu_h^2}{e(n\mu_e + p\mu_h)^2}$$

where *n* and *p* are the electron and hole densities, and μ_e and μ_h are the electron and hole mobilities, respectively.

For Hall effect experiments, thin samples are desirable, since for a given magnetic field B the magnitude of the Hall voltage is directly proportional to the current density. Patel, et.al. [19], studied the Hall coefficient and carrier mobility of a single crystal of GaAs under pressures up to 6 GPa by evaporating gold-germamium contacts onto a GaAs wafer, and then cleaving and polishing the wafer to obtain a sample 150 μm x 150 μm x 40 μm. Gold wires were then attached to the sample with silver epoxy, and glycerol was used as a pressure medium. The Hall coefficients and carrier mobility of GaAs were then measured to 6 GPa.

Hall effect and magnetoresistance experiments have also been performed by Boye, et.al. [20,21] on nickel samples using diamond anvil cells. Their approach is unique in that they combined lithographic and electroplating techniques to produce free—standing $Ni_{0.985}O_{0.015}$ thin film samples having precise dimensions and geometry. The samples measured 50 μm x 50 μm x 15 μm and pressure contact was made to four 125 mm diameter Pt wires using a pyrophyllite piece. Hall coefficient and magnetoresistance experiments were performed to pressures up to 6 GPa using 10 Tesla magnetic fields. A decrease in the high field magnetoresistance was attributed to a reduction in electron–magnon scattering due to spin wave damping under high magnetic fields.

Photoconductivity

High pressure photoconductivity data is sometimes used to complement electrical resistivity data when studying materials which may be in the vicinity of an expected insulator-to-metal transition. Photoconductivity can be a convenient add-on experiment since the major difficulties associated with setting up a conductivity experiment have already been overcome, and only a small additional investment in time and equipment (e.g.,an illumination laser, optical chopper, lock-in amplifier) is needed to perform photoconductivity experiments. In a resistivity experiment on hydrogen to 210 GPa which showed no measurable conduction to 210 GPa, for example, Eremets, et. al., [22] looked for evidence of small hydrogen bandgap by illuminating the sample with a 647 nm laser (1.9 eV) while monitoring the conductance of the sample. No measurable photoconductivity was observed, indicating that the bandgap was still above 1.9 eV at 210 GPa.

Photoconductivity as well as resistivity experiments were also performed on hydrogen iodide (HI) under high pressure by van Straaten and Silvera [23]. Here photoconductivity measurements with a 10 mW green laser (5145 Å) were used to confirm the onset of HI metallization by band-overlap at 45 GPa.

Other Uses of Electrical Transport Techniques

Electrical transport techniques have also been used to develop a wide range of diagnostic tools for applications such as the measurement of specific heats, magnetic susceptibilities, and thermoelectric powers under high pressures. These techniques rely on the ability of electrical circuits within the sample chamber to detect changes in temperature (e.g., using thermocouple or resistive sensors), to detect induced voltages, or to transport electrical power.

Specific heat experiments with diamond anvil cells are difficult because of the highly nonadiabatic nature of the sample environment. The diamond anvils sandwiching the sample are outstanding thermal conductors, and the small size of the sample chamber means that any thermal insulating layer must be rather thin, perhaps not more than a few microns thick. Coupled with the small size of the sample, this means that the thermal relaxation time of the sample is very fast, perhaps in the neighborhood of a millisecond or less. Consequently, in order to detect changes in the specific heat of the sample, ac calorimetry methods are required in which thermal power to the sample is varied at a very rapid frequency of several kHz or more while the magnitude of the sample's temperature oscillations is monitored.

D. Braithwaite, et. al. [24], developed a high pressure specific heat technique in which a pair of Au/Au-Fe thermocouples was introduced into the sample chamber to measure the sample temperature while it was heated by a series of laser pulses delivered via an optic fiber. A lock-in amplifier was used to detect the temperature oscillations at the frequency of the chopped laser. The experimental setup is shown in Figure 8. Figure 9

shows a peak in the specific heat of a $Sr_{2.5}Ca_{11.5}Cu_{24}O_{41}$ sample going through an antiferromagnetic phase transition.

A magnetic susceptibility technique developed by Alireza and Julian [25] involved placing a small wire signal coil inside the sample chamber (Figure 10). The signal coil was made of 12 μm diameter copper wire which was wound into a coil just 300 μm in diameter. This technique results in a very high sample filling factor with the size of the coil very well matched to the size of the sample. A magnetic excitation coil outside of the sample chamber was used to generate an alternating magnetic field, and magnetic induction then generates a voltage in the signal coil inside the sample chamber, with the magnitude of the induced voltage varying with the magnetic susceptibility of the sample. Because of the high sensitivity and low noise level of the sensing coil, it has also been successfully used to perform de Haas – van Alphen (dHvA) experiments at high pressure [26]. In these experiments, small oscillations in the magnetic susceptibility of a sample as a function of applied magnetic field are used to gain information on extremal cross-sectional areas of Fermi surfaces.

Thermoelectric power experiments have also been performed with diamond anvil cells by Polvani, et. al., [27] by introducing a pair of thermocouples into the sample chamber in order to measure the average temperature gradient along the length of a small sample (Figure 11). Good electrical as well as thermal contact between the thermocouple junctions and the sample is required, since the thermocouples are used to measure both the voltage gradient as well as the temperature gradient along the sample. The temperature gradient is established by heating one end of the long sample with an infrared laser.

The ability to place electrical wires leading to the sample chamber also offers the possibility of transporting large amounts of electrical power to heat samples to high temperatures [13,14 ,15]. These internal resistive heating methods are capable of reaching sample temperatures of thousands of degrees, but it has proved difficult to reach pressures of more than about 20 – 30 GPa because the electrical wires are susceptible to breaking or short-circuiting as the wires, insulating layers, and gasket deform under high pressure loading. Since it is difficult to introduce much thermal insulation between the internal resistive heating element and the diamond anvils, considerable amounts of electrical power and electrical current must be delivered to the sample. Recently, Zha and Bassett [28] have performed internal resistive heating experiments examining the high pressure melting temperature of gold samples embedded in small rhenium wires. More recent work involving a modification of their original technique was successful in measuring the P-V-T equation-of-state of platinum to pressures of 80 GPa and temperatures up to 1900 K [29].

Future Directions

High pressure electrical transport experiments have provided much valuable data on the electronic properties of materials under high pressure including the discovery of unexpected superconducting phases. However, research progress in this area has been hampered by the fact that setting up an electrical transport experiment can be very difficult and time consuming. Electrical experiments at Mbar pressures are extremely difficult and remain the preserve of just a few talented experimentalists.

In recent years, several research groups have been turning to modern microfabrication technologies to build electrical circuits within the diamond anvils themselves. Efforts thus far have involved either using boron ion implantation to 'write' electrically conductive paths in the diamond anvil, or lithographic techniques to deposit a metal thin-film circuit onto the diamond surface followed by chemical vapor deposition (CVD) of a protective diamond film over the circuit. Among other advantages, these microfabrication approaches offer the experimentalist the convenience of working with anvils which are already pre-wired and electrically insulated, thus overcoming some of the greatest problems associated with setting up high pressure electrical transport experiments. The ability to precisely control the circuit layout may also lead to further advanced development of some of the diagnostic techniques discussed earlier which utilize electrical circuits placed on diamond anvils such as specfic heat, thermoelectric power, magnetic susceptibility, and de Haas – van Alphen.

Acknowledgements

This work performed under the auspices of the U.S. Department of Energy by Lawrence Livermore National Laboratory under Contract DE-AC52-07NA27344.

Figure Captions

Figure 1. Various techniques for electrically insulating electrical wires from the gasket. (a) Mica gasket with MgO insulator assembly of R. Reichlin [1]. (b) Metal gasket with an alumina insulating layer assembly of Gonzalez and Besson [2].

Figure 2. (a) Assembly of the iron conductivity experiment of Shimizu, et. al. [10]. (b) The resistivity of iron versus temperature at 25 GPa, showing a drop in resistivity below 1 K attributed to superconductivity.

Figure 3. The resistivity of an iron sample at 25 GPa under various magnetic field strengths [10].

Figure 4. A phase diagram indicating the superconducting region of iron found in the experiments of Shmizu, et. al. [10].

Figure 5. Assembly for a high-pressure conductivity experiment on oxygen by Shimizu, et. al. [12].

Figure 6. Normalized resistance of an oxygen sample under various magnetic field strengths [12].

Figure 7. (a) Resisitivity versus pressure of a single-crystal sample of tetramethyltetratelluronaphtalene (TMTTeN) to 30 GPa. The inset shows the single-crystal sample with attached wires at a pressure of 25 GPa. (b) Temperature dependence of the resistivity of TMTTeN at various pressures.

Figure 8. The experimental setup for high-pressure specific heat experiments by Braithewaite, et. al., [24] showing the thermocouple assembly used for monitoring temperature variations in a sample as it is pulse heated with a laser.

Figure 9. Specific heat of a $Sr_{2.5}Ca_{11.5}Cu_{24}O_{41}$ sample as a function of temperature using the DAC specific heat technique of Braithewaite, et. al. [24]

Figure 10. (a) High-pressure magnetic susceptibility assembly of Alireza and Julian [], showing the placement of the excitation, compensation, and sensing coils. (b) A picture of a sensing coil made from 12 μm insulated copper wire.

Figure 11. (a) Thermoelectric power measurement assembly of Polvani, et. al. [27] showing the pair of thermocouple junctions used to measure the temperature gradient along the length of the sample. (b) Schematic diagram of the overall DAC assembly.

Figures

Figure 1.

(a)

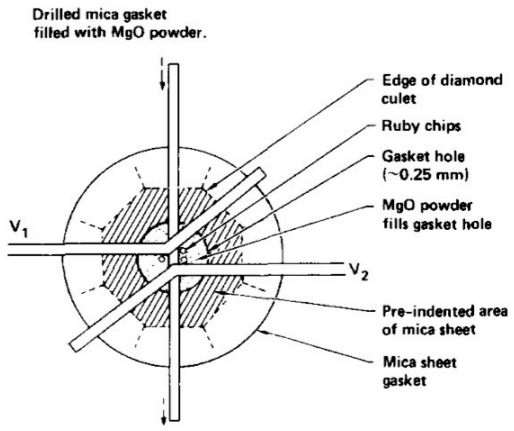

(b)

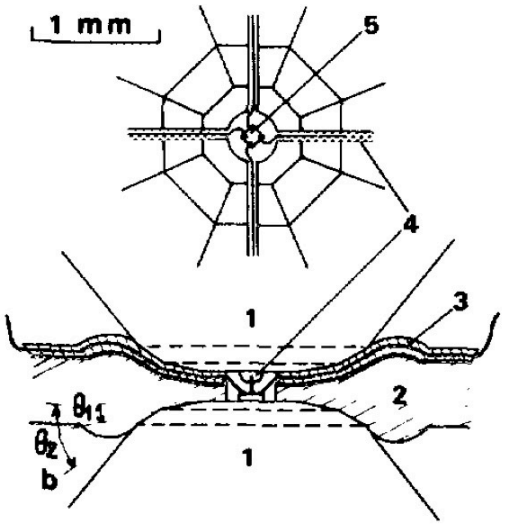

Figure 2.

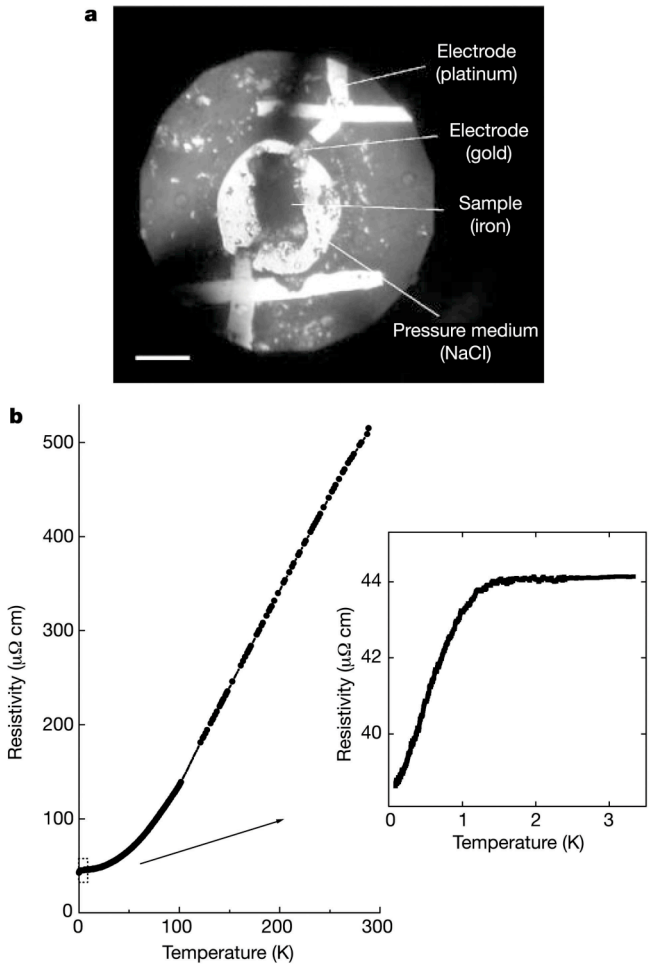
a
Electrode
(platinum)
Electrode
(gold)
Sample
(iron)
Pressure medium
(NaCl)
b
Resistivity (μΩ cm)
Temperature (K)
Resistivity (μΩ cm)
Temperature (K)

Figure 3.

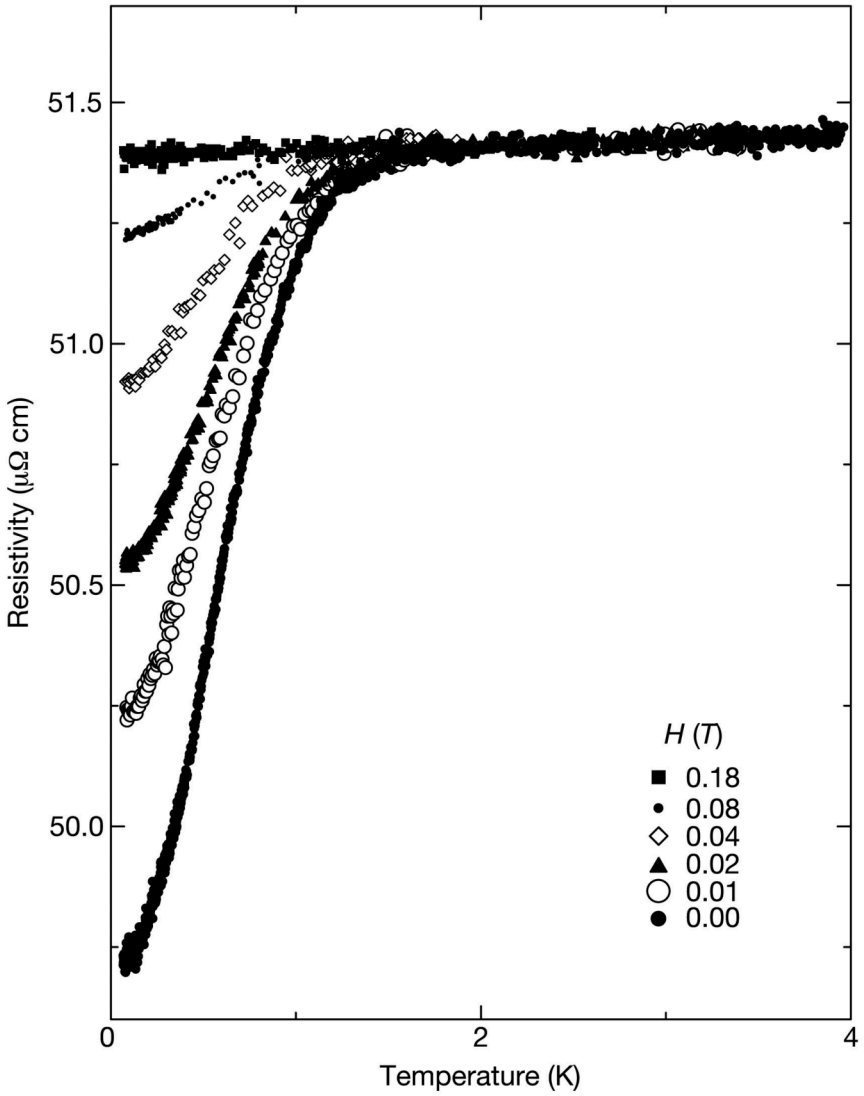
51.5
51.0
50.5
50.0
Resistivity (μΩ cm)
0
2
4
Temperature (K)
H (T)
0.18
0.08
0.04
0.02
0.01
0.00

Figure 4.

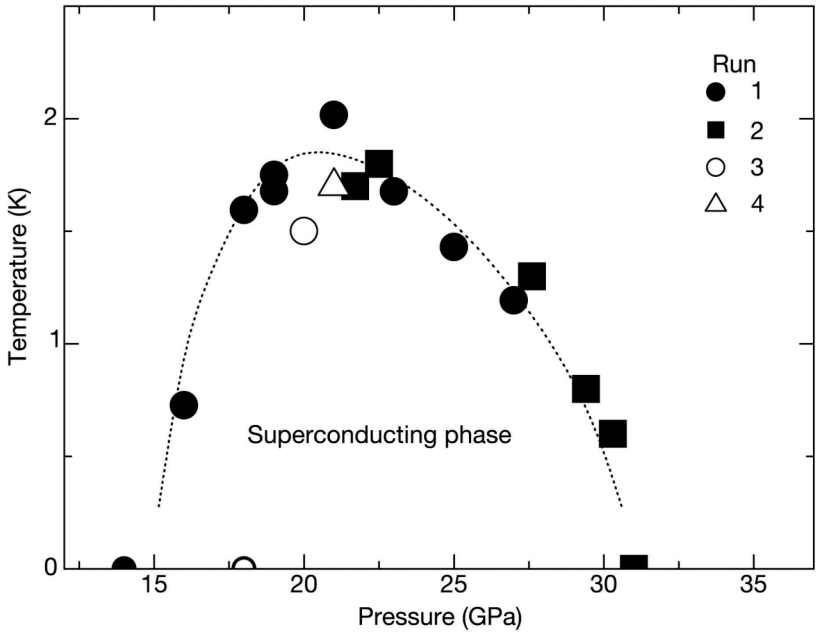
Run
1
2
3
4
Temperature (K)
Pressure (GPa)
Superconducting phase
0
1
2
15
20
25
30
35

Figure 5.

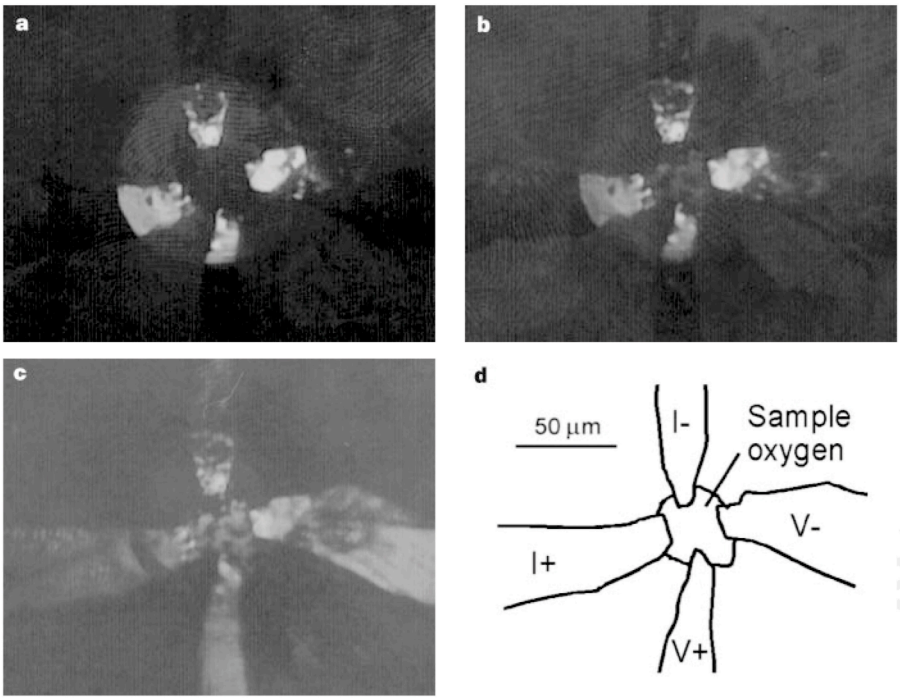

Figure 6.

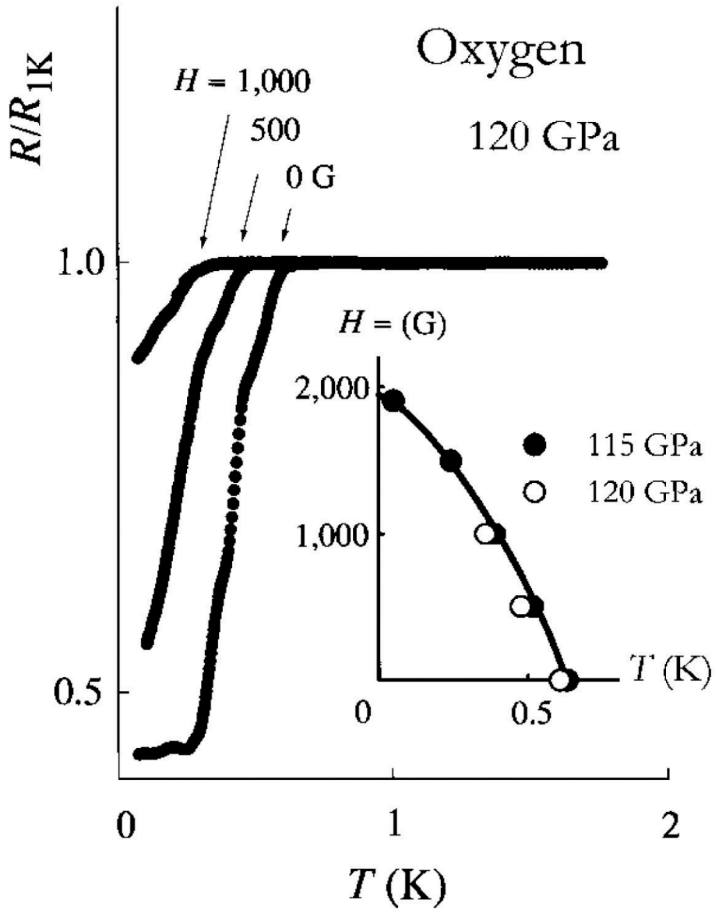
Oxygen
120 GPa
H = 1,000
500
0 G
R/R1K
1.0
0.5
0
1
2
T (K)
H = (G)
2,000
1,000
0
0.5
T (K)
115 GPa
120 GPa

Figure 7.

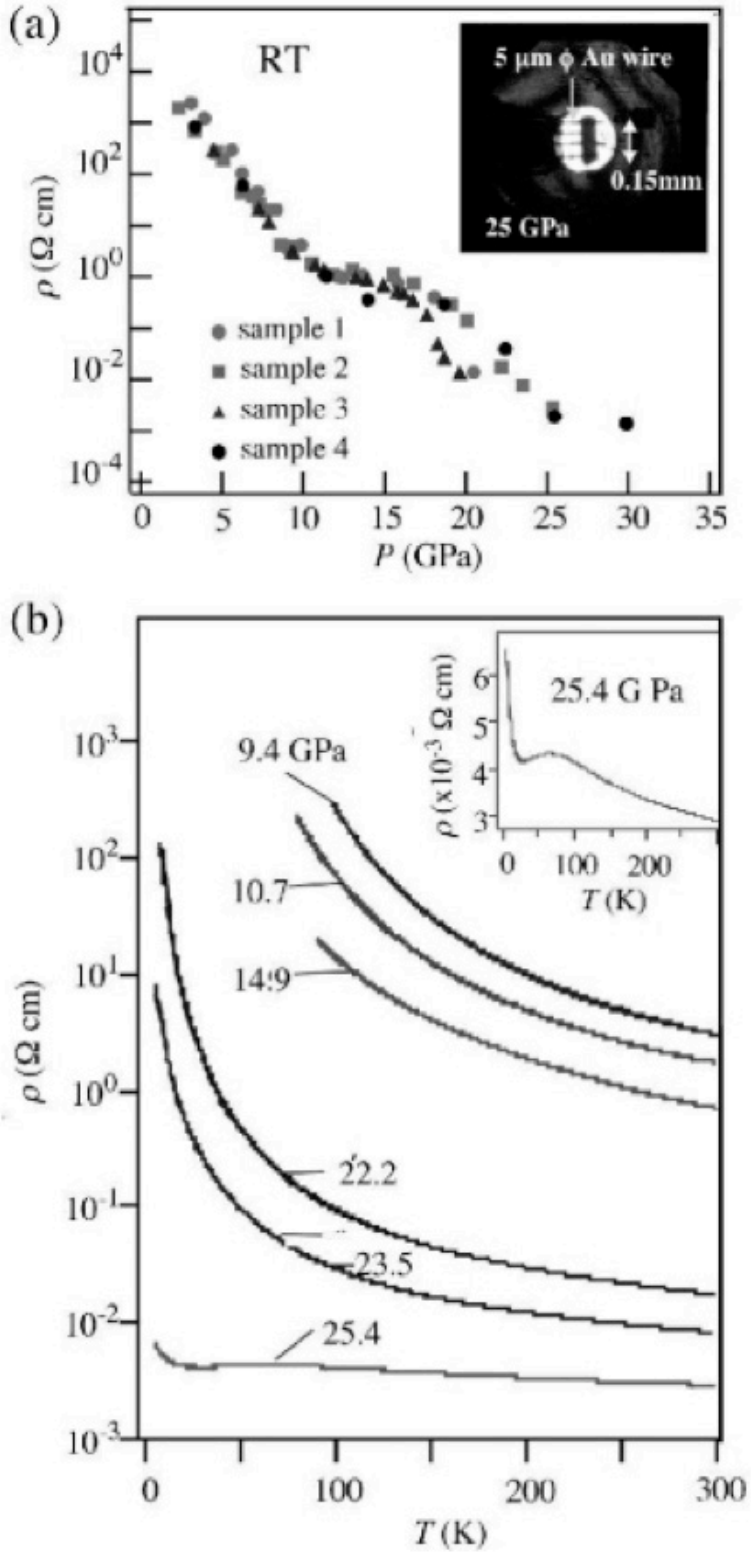
(a)
RT
5 μm ϕ Au wire
0.15mm
25 GPa
sample 1
sample 2
sample 3
sample 4
ρ (Ω cm)
P (GPa)
(b)
9.4 GPa
10.7
14.9
22.2
23.5
25.4
25.4 G Pa
ρ (x10⁻³ Ω cm)
T (K)
ρ (Ω cm)
T (K)

Figure 8.

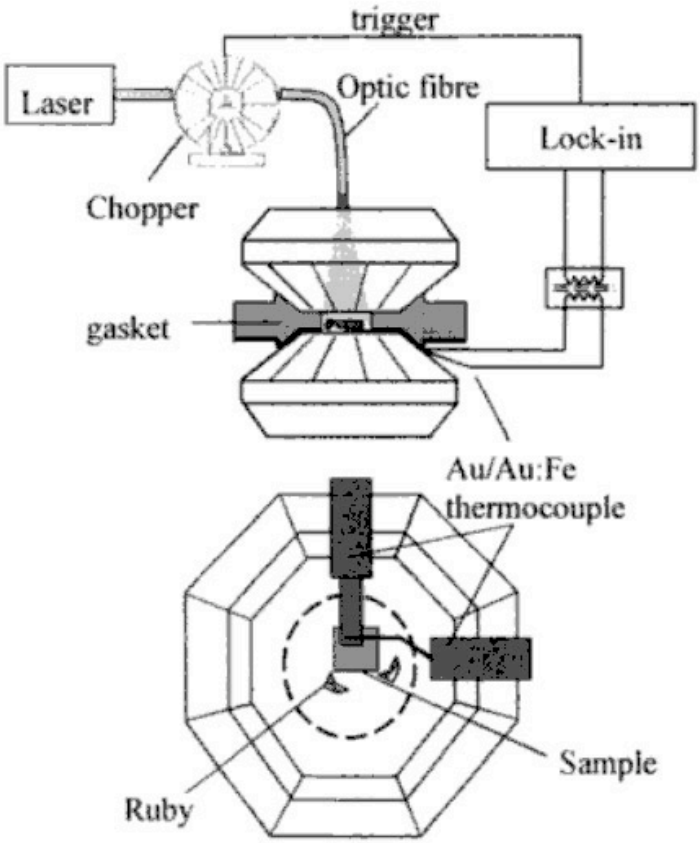
trigger
Laser
Optic fibre
Lock-in
Chopper
gasket
Au/Au:Fe
thermocouple
Sample
Ruby

Figure 9.

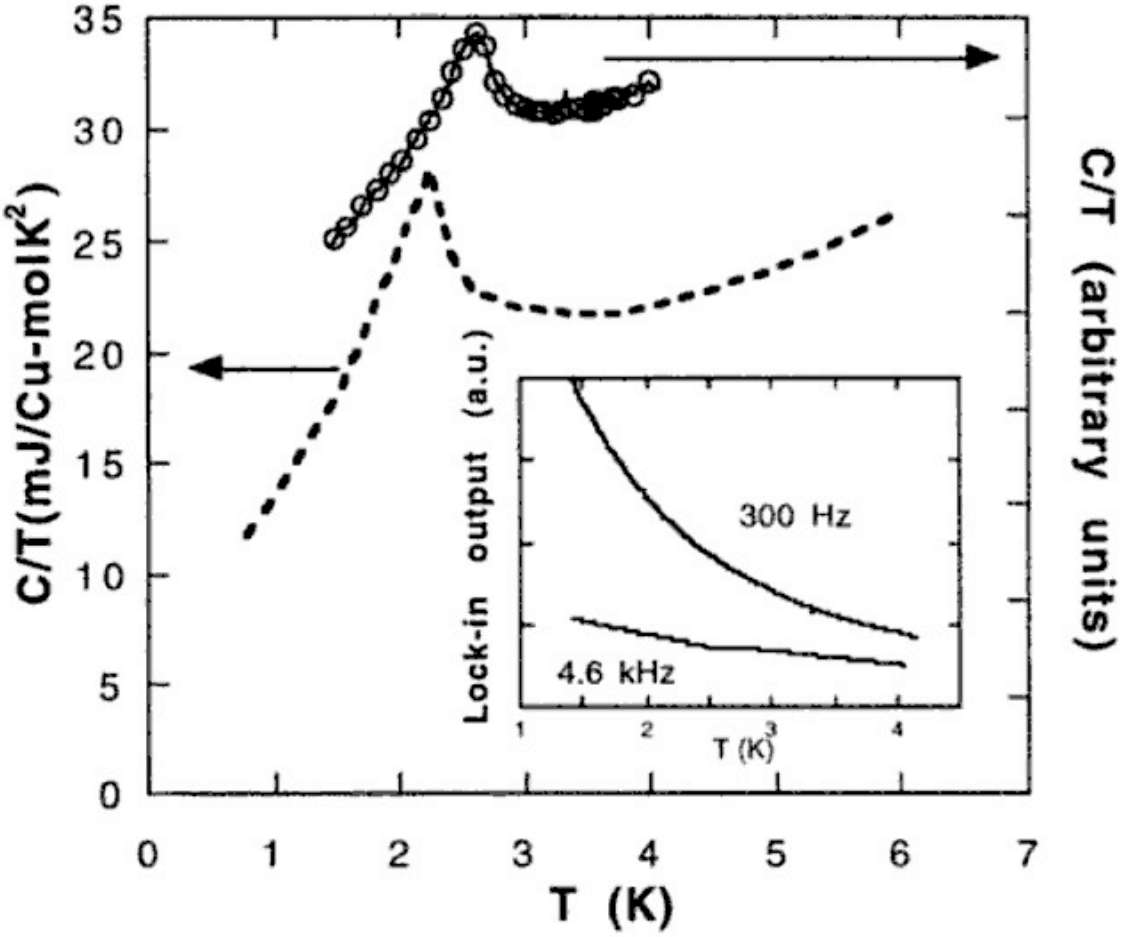
C/T(mJ/Cu-molK²)
C/T (arbitrary units)
T (K)
Lock-in output (a.u.)
300 Hz
4.6 kHz
T (K)³

Figure 10.

(a)

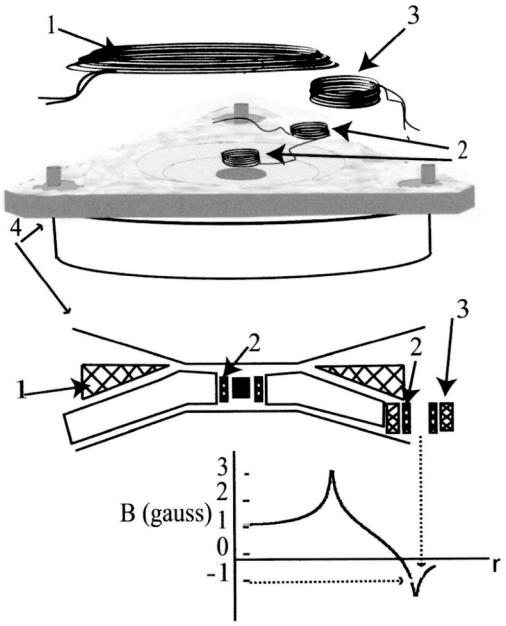

(b)

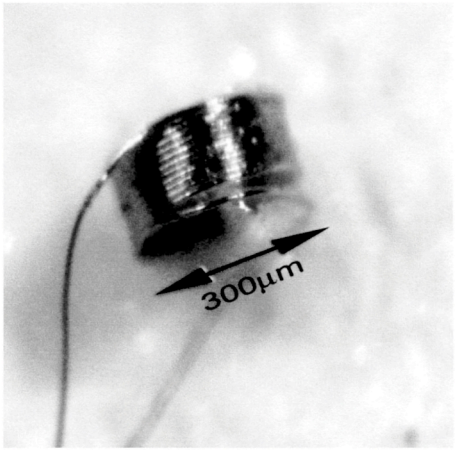

Figure 11.

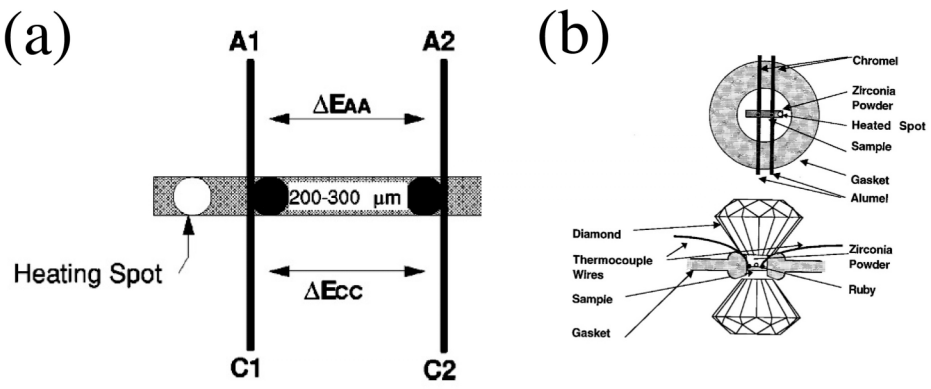
(a)
A1
A2
ΔEAA
200-300 μm
Heating Spot
ΔEcc
C1
C2
(b)
Chromel
Zirconia Powder
Heated Spot
Sample
Gasket
Alumel
Diamond
Thermocouple Wires
Sample
Gasket
Zirconia Powder
Ruby

1. Reichlin, R.L., Measuring the electrical resistance of metals to 40 GPa in the diamond-anvil cell, *Rev. Sci. Instrum*. 54, 1674, 1983.
2. Gonzalez, J., Besson, J.M., and Weill, G., Electrical transport measurements in a gasketed diamond anvil cell up to 18 GPa, *Rev. Sci. Instrum*. 57, 106, 1986.
3. Eremets M.I., Struzhkin, V.V., Mao H.-K., and Hemley, R.J., Superconductivity in Boron, *Science*, 293, 272, 2001.
4. Grzybowski, T.A., and Ruoff, A.L., Band-overlap metallization of BaTe, *Phys. Rev. Lett*., 53, 489, 1984.
5. Hemmes, H, Driessen, A., Kos, J., Mul, F.A., Griessen, R., Synthesis of metal hydrides and in situ resistance measurements in a high-pressure diamond anvil cell, *Rev. Sci. Instrum*., 60, 474, 1989.
6. Bureau, H., Burchard, M., Kubsky, S., Henry, S., Gonde, C., Zaitsev, A., and Meijer, J., Intelligent anvils applied to experimental investigations: state-of-the-art, *High Pressure Research*, 26, 251, 2006.
7. Weir, S.T., Akella, J., Aracne-Ruddle, C., Vohra, Y.K., Catledge, S.A., Epitaxial diamond encapsulations of metal microprobes for high pressure experiments, *Appl. Phys. Lett*., 77, 3400, 2000.
8. van der Pauw, L.J., *Philips Res. Rep*., 13, 1, 1958.
9. Huang, X., Gao, C., Han, Y., Li, M., He, C., Hao, A., Zhang, D., Yu, C., Zou, G., and Ma, Y., Finite element analysis of resistivity measurement with van der Pauw method in a diamond anvil cell, *Appl. Phys. Lett*., 90, 242102, 2007.
10. Shimizu, K., Kimura, T., Furomoto, S., Takeda, K., Kontani, K., Onuki, Y., Amaya, K., Superconductivity in the non-magnetic state of iron, *Nature* 412, 316, 2001.
11. Desgreniers, S., Vohra, Y.K., and Ruoff, A.L., Optical response of very high density solid oxygen to 132 GPa, *J. Phys. Chem.* 94, 1117, 1990.
12. Shimizu, K., Suhara K., Ikumo, M., Eremets, M.I., and Amaya, K., Superconductivity in oxygen, *Nature*, 393, 767, 1998.
13. Liu, L., and Bassett, W.A., The melting of iron up to 200 kbar, *J. Geophys. Res*., 80, 3777, 1975.
14 Mao, H.K., Bell, P.M., and Hadidiacos, C., Experimental phase relations of iron to 360 kbar, 1400 ˚C, determined in an internally heated diamond-anvil apparatus, in *High Pressure Research in Mineral Physics*, Manghnani, M.H., and Syono, Y., Eds., Terra Scientific, Tokyo, 1987, 135.
15 Boehler, R., Nicol, M., and Johnson, M.L., Internally-heated diamond anvil cell: phase diagram and P-V-T of iron, in *High Pressure Research in Mineral Physics*, Manghnani, M.H., and Syono, Y., Eds., Terra Scientific, Tokyo, 1987, 173.
16. Knittle, E., and Jeanloz, R., High-pressure metallization of FeO and implications for the earth's core, *Geophys. Res. Lett*., 13, 1541, 1986.
17 Li, M., Gao, C-X, Ma, Y., Hao, A., He, C., Huang, X., Li., Y., Liu, J., Liu, H., and Zou, G., In situ HPHT resistance measurement of $(Fe_{0.125}, Mg_{0.875})_2SiO_4$ in a designed laser heated diamond anvil cell, *J. Phys.: Condens. Matter*, 19, 1, 2007.
18. Cui, H., Okano, Y., Zhou, B., Kobayashi, A., and Kobayashi, H., Electrical resistivity of tetramethyltetratelluronaphtalene crystal at very high pressures –

examination of the condition of metallization of π molecular crystal, *J. Am. Chem. Soc*., 130, 3738, 2008.
19. Patel, D., Crumbaker, T.E., Sites, J.R., and Spain, I.L., Hall effect measurement in the diamond anvil high-pressure cell, *Rev. Sci. Instrum*., 57, 2795, 1986.
20. Boye, S.A., Rosen, D., Lazor, P., and Katadjiev, I., Precise magnetoresistance and Hall resistivity measurements in the diamond anvil cell, *Rev. Sci. Instrum*., 75, 5010, 2004.
21. Boye, S.A., Lazor, P., and Ahuja, R., Magnetoresistance and Hall effect measurements of Ni to 6 GPa*, J. Magn. Magn. Mater*., 294, 347, 2005.
22. Eremets, M.I., Struzhkin, V.V., Mao, H-K., Hemley, R.J., Exploring superconductivity in low-Z materials at megabar pressures, *Physica B*, 329-333, 1312, 2003.
23. van Straaten, J., and Silvera, I.F., Observation of metal-insulator and metal-metal transitions in hydrogen iodide under pressure, *Phys. Rev. Lett*., 57, 766, 1986.
24. Braithwaite, D., Thomasson, J., Salce, B., Nagata, T., Sheikin, I., Fujino, H., Akimitsu, J., and Flouquet, J., Coexistence of antiferromagnetic order and superconductivity in the spin ladder system $Sr_{2.5}Ca_{11.5}Cu_{24}O_{41}$, in *Frontiers of High Pressure Research II*, Hochheimer, H.D., Kuchta, B., Dorhout, P.K., and Yarger, J.L., Eds., Kluwer Academic, Dordrecht, 2001, 383.
25. Alireza, P.L., and Julian, S.R., Susceptibility measurements at high pressures using a microcoil system in a diamond anvil cell, *Rev. Sci. Instrum*., 74, 4728, 2003.
26. Goh, S.K., Alireza, P.L., Mann, P.D.A., Cumberlidge, A.M., Bergemann, C., Sutherland, M., and Maeno, Y., High pressure de Haas – van Alphen studies of Sr2RuO4 using an anvil cell, *Current Appl. Phys*., 8, 304, 2008.
27. Polvani, D.A., Meng, J.F., Hasegawa, M., and Badding, J.V., Measurement of the thermoelectric power of very small samples at ambient and high pressures, *Rev. Sci. Instrum.*, 70, 3586, 1999.
28. Zha, C-S., Bassett, W.A., Internal resistive heating in a diamond anvil cell for in situ x-ray diffraction and Raman scattering, *Rev. Sci. Instrum*., 74, 1255, 2003.
29. Zha, C-S., Mibe, K., Bassett, W.A., Tschauner, O., Mao, H-K., Hemley, R.J., P-V-T equation of state of platinum to 80 GPa and 1900 K from internal resistive heating/x-ray diffraction measurements, *J. Appl. Phys*., 103, 54908, 2008.